Chemometric Studies on the Bactericidal Activity of Quinolones via an Extended VolSurf Approach

Giovanni Cianchetta,[†] Raimund Mannhold,[‡] Gabriele Cruciani,*[,§] Massimo Baroni,[||] and Violetta Cecchetti[†]

Dipartimento di Chimica e Tecnologia del Farmaco, Università di Perugia, Via del Liceo 1, I-06123 Perugia, Italy, Department of Laser Medicine, Molecular Drug Research Group, Heinrich-Heine-Universität, Universitätsstrasse 1, 40225 Düsseldorf, Germany, Dipartimento di Chimica, Laboratorio di Chemiometria, Università di Perugia, Via Elce di Sotto, 10, I-06123 Perugia, Italy, and Molecular Discovery Ltd., 4, Chandos Street, W1A 3BQ, London, United Kingdom

Received August 5, 2003

An extended VolSurf approach, that additionally includes SHAPE descriptors, was applied to a dataset of 55 quinolones. Bactericidal activity was measured at Bayer AG, Germany, for Gram-negative (*Escherichia coli* and *Pseudomonas aeruginosa*) and Gram-positive bacteria (*Staphylococcus aureus* and *Enterococcus faecalis*). Chemometric analysis was first approached via a classical VolSurf approach. The following descriptors were found most important: bactericidal activity particularly increases with high values of the best volume ($BV11_{OH2}$) and the minimum energy ($Emin1_{OH2}$) of the water probe, high values of the integy moment (ID_{DRY}) of the lipophilic probe, and high values of the hydrophilic region (W_O) of the hydrogen bond acceptor probe. Best volume ($BV31_{OH2}$) of the water probe and best volume ($BV12_{DRY}$) and lipophilic regions (D_{DRY}) of the lipophilic probe as well as H-bonding capacity derived with the CO probe (HB_O) are inversely related to activity. PLS analysis yields a five-component model with an r^2 of 0.83 and a q^2 of 0.43 after variable selection via fractional factorial design (FFD). Chemometric modeling could be improved by including newly derived SHAPE descriptors, which were merged with the VolSurf descriptors and subjected to PLS analysis. The global model of this extended VolSurf approach is optimal with two components and exhibits a significantly improved statistical quality; a marginally reduced r^2 (0.75 versus 0.83) is more than compensated by a highly improved predictivity with a q^2 of 0.63 versus 0.43. To prove model quality, external prediction of seven test set quinolones was performed. The precise prediction of all test set molecules nicely demonstrates the robustness and statistical significance of the obtained chemometric model using the extended VolSurf approach.

Introduction

Quinolones are highly potent, orally active antibacterials. They inhibit DNA synthesis by interacting with two essential bacterial type II topoisomerases, DNA gyrase, and topoisomerase IV.[1−4] Both enzymes play crucial, but distinct, roles during DNA replication despite a high degree of similarity in their structure and functions.[5] They catalyze the passage of a double strand region of DNA through a transient double strand break in the helix and resealing the break. DNA gyrase acts primarily to solve topological problems during DNA replication and to relieve the positive supercoiling accumulated during DNA transcription. Topoisomerase IV is required at the terminal stages of DNA replication for unlinking newly replicated daughter chromosomes.[2] Quinolones inhibit enzyme function by binding to the catalytic intermediate enzyme−DNA complex.[1−4] The stabilization of the resulting quinolone−enzyme−DNA complex leads to the generation of double-strand DNA breaks that trigger a cascade of events leading to cell death.[1,2] The molecular organization of the complex is presently unknown although several models have been suggested.[6−8] Quinolones differ in their relative activities against DNA gyrase and topoisomerase IV.[1]

Since the discovery of the first antibacterial quinolone, nalidixic acid,[9] the molecular structures of quinolones have been extensively modified to improve their antimicrobial properties and pharmacokinetic profile.[10−12] A main modification was the introduction of a C6-fluorine atom. Fluoroquinolones, clinically applied since the mid-1980s, are widely used for the treatment of various bacterial infections of the lower respiratory tract, urinary tract, and skin/soft tissue, as well as sexually transmitted diseases. However, their potency against a number of clinically important Gram-positive bacteria and anaerobes is limited.[10,13,14]

The next significant advance represent recently marketed fluoroquinolones such as gatifloxacin,[15] moxifloxacin,[16] and gemifloxacin[17] which exhibit an improved bactericidal activity against Gram-positive bacteria (particularly pneumococcus including penicillin-resistant strains) and anaerobes without any decrease in their Gram-negative spectrum or alterations in their pharmacological profile.[12,18]

However, the extensive clinical use of fluoroquinolones resulted in an increased quinolone resistance among many pathogens.[19−21] In addition, certain adverse events (e.g. CNS, phototoxicity, and arthropathy) became apparent, although the more serious events are rare.[22,23] Thus, despite many advances in the fluoroquinolone

* Corresponding author. Phone: +39 075 5855550. Fax: +39 075 45646. E-mail: gabri@chemiome.chm.unipg.it.
[†] Dipartimento di Chimica e Tecnologia del Farmaco, Università di Perugia.
[‡] Heinrich-Heine-Universität.
[§] Dipartimento di Chimica, Università di Perugia.
[||] Molecular Discovery Ltd.

10.1021/jm030986y CCC: $27.50
Published on Web 05/07/2004

Chart 1. Quinolone Core with Main Substitution Sites

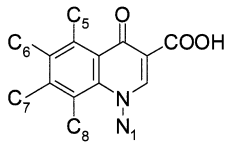

field, there exists continuous need for novel quinolones to overcome the limitations of existing drugs.

Correspondingly, the present study is dedicated to derive chemometric models for a dataset of quinolones via an extended VolSurf approach, the first time described here. Extension refers to the inclusion of SHAPE descriptors. Robustness of the achieved models is investigated via external prediction of some test set quinolones.

Results and Discussion

A plethora of papers deals with structure−activity relationships of quinolones referring to potency, pharmacokinetic properties, and side effects.[4,24−27] The 1,4-dihydro-4-oxopyridine-3-carboxylic acid associated with a 5,6-fused aromatic ring is the common chemical feature of bactericidal quinolones (Chart 1). In the resulting bicyclic ring, the 1-, 5-, 6-, 7-, and 8-positions are the major targets of chemical variation. N-1 position: Hydrophobic substituents are essential. They have some impact on pharmacokinetics and control overall potency; cyclopropyl is optimal. C-5 position: Small hydrogen bond donor or acceptor substituents are allowed; specific moieties at C-5 increase activity against Gram-positive bacteria. C-6 position: Almost all clinically useful quinolones bear a fluorine at C-6; it increases the inhibitory activity against DNA gyrase and improves the penetration into the bacterial cell. C-7 position: Synthetic efforts for improved potency has been the main focus here; both activity spectrum and kinetic profile can be controlled at C-7. Five- or six-membered N-heterocycles promote excellent antibacterial properties. C-8 position: Substituents need to be small; kinetic profile and activity versus anaerobic bacteria can be adjusted through substitution at C-8.

In recent years, structural innovations in the quinolone antibacterial field have been reported such as the nonfluorinated quinolones[28] and the 2-pyridones.[29] They do not fit within the above SAR but may expand the quinolone SAR into productive new areas.

QSAR studies on quinolones are quite limited as compared to the qualitative investigations mentioned above.[30−35] To enable a rapid, statistically robust and easily interpretable approach, we describe here an extended VolSurf methodology. Corresponding chemometric analysis was applied to a database of 55 quinolones including the marketed moxifloxacin **02**, levofloxacin **03**, norfloxacin **04**, ciprofloxacin **05**, sparfloxacin **34**, lomefloxacin **44**, and pefloxacin **45** (Chart 2).

Bactericidal activity (Table 1) was measured at Bayer AG, Wuppertal, Germany, in Gram-negative (*Escherichia coli* and *Pseudomonas aeruginosa*) as well as Gram-positive bacteria (*Staphylococcus aureus* and *Enterococcus faecalis*). Bactericidal potency is often expressed as minimum inhibitory concentration MIC, which is the lowest antibiotic concentration that visibly inhibits growth of microorganisms after in vitro incubation, at a time when an untreated culture becomes readibly visible in or on culture medium. MIC is expressed in terms of 100% inhibition and given in μg/mL. To reflect differences in molecular weight, we use molar MIC-values in their reciprocal logarithmic form (log 1/*C*). In *E. coli*, the bactericidal activity ranges from a log 1/*C* of 8.06 for the most potent compound **28** to a log 1/*C* of 3.43 for the weakest compound **35** and covers a spectrum of 4.6 log units. In *P. aeruginosa*, a somewhat smaller spanned activity space of 3.4 log units is observed, ranging from a log 1/*C* of 6.84 for compound **46** to a log 1/*C* of 3.43 for compound **35**. Observed activities in *P. aeruginosa* are up to two log units lower than in the remaining test systems. In *S. aureus*, the spanned activity space is identical to that found in *E. coli*; most potent and weakest compound coincide as well. In *E. faecalis*, the activity space spans 4.3 log units with compound **37** exhibiting the highest (log 1/*C* = 7.73) and compound **35** the weakest activity (log 1/*C* = 3.43).

To derive QSAR models for the above-described quinolones, we started with the VolSurf approach, which is well accepted in chemometric science to adequately cope with complex biological data involving a significant impact of kinetic properties as commonly present in cell systems such as those used for characterizing the quinolones included here.

In a first step, VolSurf descriptors were derived using the water (OH2), the lipophilic (DRY), and the hydrogen bond acceptor probe (O) and in turn subjected to a comparative PLS analysis including the activities in all four test systems. The PLS loadings plot in Figure 1 demonstrates that the chemical descriptors with the highest impact on the variance in bactericidal activity are nearly the same in the four test systems. This can be derived from the almost identical projection of the four activities in this plot. Coincidence is particularly evident for Gram-positive bacteria (Y3 and Y4), whereas marginal differences are observed for Gram-negative bacteria (Y1 and Y2).

The quasi-identical projection of the four individual Y's allowed us to develop a global PLS model which exhibits significant advantages over individual models. The correlation on the individual Y's can be used by PLS to increase the signal-to-noise ratio and to derive a more robust model. To derive such a global PLS model, a consensus Y was constructed, applying principal component analysis (PCA) to the four individual Y's. PCA scores of the first component served as the new consensus Y. Corresponding PLS analysis yielded a five-component model with an r^2 of 0.83 and a q^2 of 0.43 after variable selection via fractional factorial design (FFD).

The VolSurf descriptors with the strongest impact on bactericidal activity are highlighted in a PLS coefficients plot in Figure 2. Activity particularly increases with high values of the best volume ($BV11_{OH2}$) and the minimum energy interaction ($Emin1_{OH2}$) of the water probe, with high values of the integy moment (ID_{DRY}) of the lipophilic probe and with high values of the hydrophilic region (W_O) of the hydrogen bond acceptor probe. Best hydrophilic volumes refer to the largest water and hydrophilic regions (W_O) accessible surface area. Dense and localized polar regions markedly favor bactericidal activity. Conversely best volume ($BV31_{OH2}$) of the water probe, best volume ($BV12_{DRY}$) and lipophilic

Chart 2. Chemical Structures of the Quinolone Training Set ($n = 55$)[a]

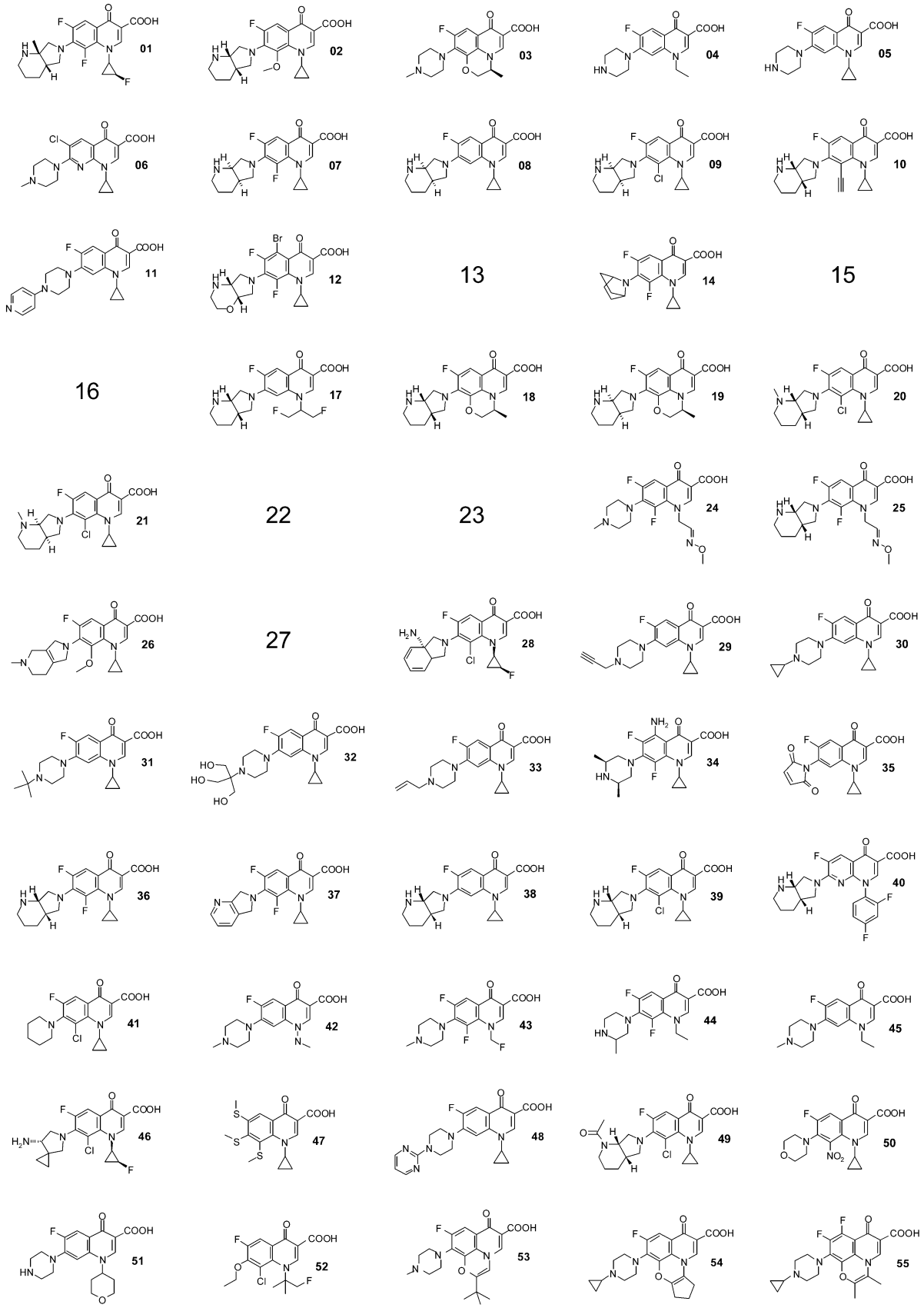

[a] The database includes the marketed moxifloxacin **02**, levofloxacin **03**, norfloxacin **04**, ciprofloxacin **05**, sparfloxacin **34**, lomefloxacin **44**, and pefloxacin **45**. The compounds exhibit 6-fluoro substitution with two exceptions (**06** and **47**). Main variations refer to 1- and 7-positions. All compounds were synthesized at Bayer AG, Wuppertal, Germany. Structures **13**, **15**, **16**, **22**, **23**, and **27** are not disclosed because patents are pending.

Table 1. Bactericidal Activity of the Dataset Compounds[a]

code	*Escherichia coli*	*Pseudomonas aeruginosa*	*Staphylococcus aureus*	*Enterococcus faecalis*
01	7.46	6.25	7.16	6.86
02	7.46	5.64	7.16	6.55
03	7.41	6.20	6.50	6.20
04	6.76	5.85	5.55	5.55
05	7.66	6.77	6.16	6.16
06	6.77	4.96	4.96	4.35
07	7.45	5.63	6.84	6.53
08	6.82	5.61	6.21	5.91
09	7.47	5.65	6.85	6.85
10	7.70	5.90	7.70	7.70
11	5.91	3.50	5.61	4.71
12	6.58	4.47	6.27	5.37
13	7.16	5.34	6.86	6.24
14	5.86	4.35	5.86	5.26
15	7.10	5.29	6.49	6.19
16	5.80	5.30	6.20	6.20
17	5.61	4.11	5.01	5.01
18	6.80	5.59	6.19	6.19
19	6.19	5.29	5.89	5.89
20	7.45	5.62	7.13	6.84
21	7.15	5.32	6.83	6.23
22	6.49	5.29	6.19	5.89
23	6.19	4.99	5.89	5.89
24	5.29	4.39	4.39	3.49
25	5.62	4.42	5.62	4.42
26	6.84	5.32	6.84	6.52
27	6.77	5.55	6.16	5.55
28	8.06	6.56	8.06	7.16
29	6.83	5.01	6.21	5.61
30	7.08	4.67	6.17	5.57
31	7.10	5.29	6.19	5.89
32	5.34	3.53	4.74	4.13
33	6.82	5.31	6.21	5.61
34	7.42	5.59	6.80	6.20
35	3.43	3.43	3.43	3.43
36	8.02	6.23	7.44	6.84
37	6.53	5.02	7.44	7.73
38	7.12	5.92	7.12	6.21
39	8.05	6.25	7.75	7.16
40	7.50	5.09	6.59	6.00
41	6.46	5.26	7.42	6.79
42	6.75	5.83	5.52	4.92
43	7.07	5.85	5.85	5.55
44	7.07	5.85	5.85	5.24
45	7.05	5.82	6.12	5.52
46	8.04	6.84	7.74	7.45
47	4.36	3.46	4.96	3.76
48	4.41	3.50	5.01	4.71
49	5.35	3.84	5.95	5.65
50	5.58	3.77	5.58	4.67
51	3.77	3.47	4.07	4.07
52	4.35	3.45	4.95	4.05
53	4.44	3.53	3.84	4.14
54	4.15	3.54	4.75	4.75
55	4.12	3.51	4.42	4.12

[a] Bactericidal activity is expressed as log 1/*C*. In *Escherichia coli*, activity ranges from 8.06 for **28** to 3.43 for **35**; spectrum = 4.6 log units. In *P. aeruginosa*, a smaller activity range of 3.4 log units is observed, ranging from 6.84 for **46** to 3.43 for **35**. In *S. aureus*, the spanned space is identical to that found in *E. coli*; most potent and weakest compound coincide as well. In *E. faecalis*, the activity space ranges over 4.3 log units; compound **37** exhibited the highest (log 1/*C* = 7.73) and **35** the weakest activity (log 1/*C* = 3.43). Biological data stem from Bayer AG, Germany.

regions (D_{DRY}) of the lipophilic probe and HB_O (H-bonding capacity derived with the CO probe) are inversely related to bactericidal activity. The meaning is that hydrophobic regions are not optimal for potency, but some hydrophobic regions can be tolerated provided they are strictly confined to particular surface.

To exemplify the explanatory potency of the VolSurf descriptors, they are compared for a highly potent **46** and a weakly active compound **54** in Figure 3. High values of the best volume ($BV12_{OH2}$) of the water probe, high values of the integy moment ($ID4_{DRY}$) of the lipophilic probe, and high values of the hydrophilic region ($W7_O$) of the hydrogen bond acceptor probe explain the high potency of compound **46**. The weakly active compound **54** exhibits low or even null values for these descriptors.

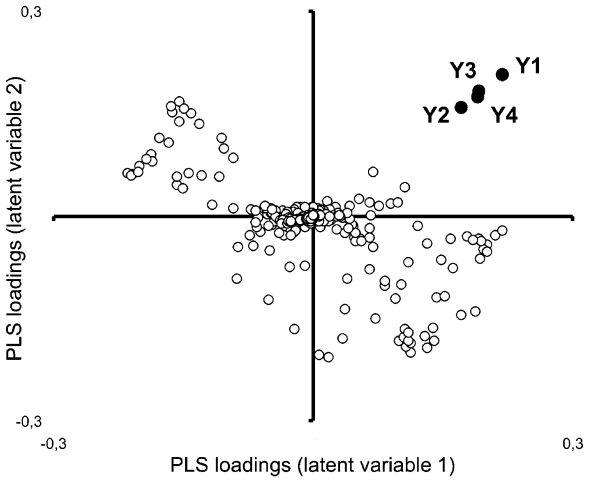

Figure 1. The PLS loadings plot demonstrates that the chemical descriptors with the highest impact on the variance in bactericidal activity are nearly the same in the four test systems (Y1−Y4). This can be derived from the almost identical projection of the four activities in this plot. Coincidence is particularly evident for Gram-positive bacteria (Y3 and Y4), whereas marginal differences are observed for Gram-negative bacteria (Y1 and Y2).

In addition to the global analysis, separate VolSurf-models were derived for the four different test systems to allow an individual analysis of the statistical quality (Table 2). PLS analysis resulted in a five-component model that explains 83% (*E. coli*), 85% (*P. aeruginosa*), 81% (*S. aureus*), and 79% (*E. faecalis*) of the variance in bactericidal activity. Activity is better explained for Gram-negative than for Gram-positive bacteria, which is particularly shown by the lower predictivity in the latter case (for q^2 values see Table 3). Interpretation and predictivity of the obtained models could be improved by variable selection via fractional factorial design. Variable selection reduced the number of descriptors from initially 92 to 67 (*E. coli*), 68 (*P. aeruginosa*), 59 (*S. aureus*) and 49 (*E. faecalis*) and increased the q^2 values to 0.50 for *E. coli*, 0.60 for *P. aeruginosa*, 0.41 for *S. aureus* and 0.43 for *E. faecalis*.

VolSurf descriptors rather comprehensively circumscribe the global properties of drug molecules. Their only minor limitation refers to the description of shape. Accordingly, we attempted to further improve the chemometric modeling by including SHAPE descriptors, which were derived with a new procedure.

Molecular shape is normally described by molecular volume function. Such function is set to 1 within the radius of each atom and 0 outside. The function's integration all over the 3D space returns the molecule volume. Typical molecular volume functions are constructed from the individual volume functions of each atom; this is not the best method because of the problem of atom overlaps.

The molecular shape function used in this paper is constructed from the probe−target interaction energies

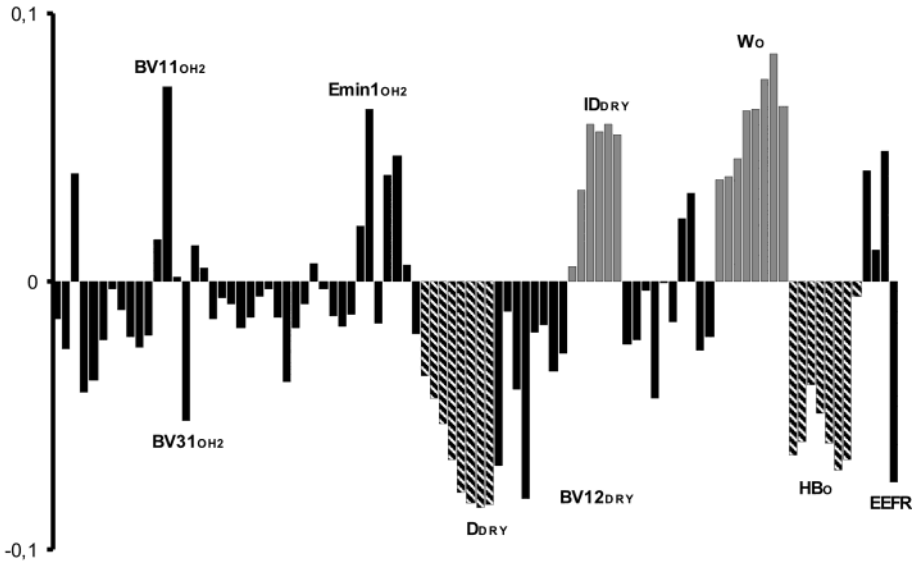

Figure 2. The PLS coefficients plot highlights the VolSurf descriptors, which are directly (positive values) or inversely (negative values) correlated to the bactericidal activity (consensus Y). Activity particularly increases with high values of the best volume ($BV11_{OH2}$) and the minimum energy ($Emin1_{OH2}$) of the water probe, high values of the integy moment (ID_{DRY}) of the lipophilic probe. and high values of the hydrophilic region (W_O) of the hydrogen bond acceptor probe. Best volume ($BV31_{OH2}$) of the water probe, best volume ($BV12_{DRY}$) and lipophilic regions (D_{DRY}) of the lipophilic probe as well as HB_O and EEFR are inversely related to activity.

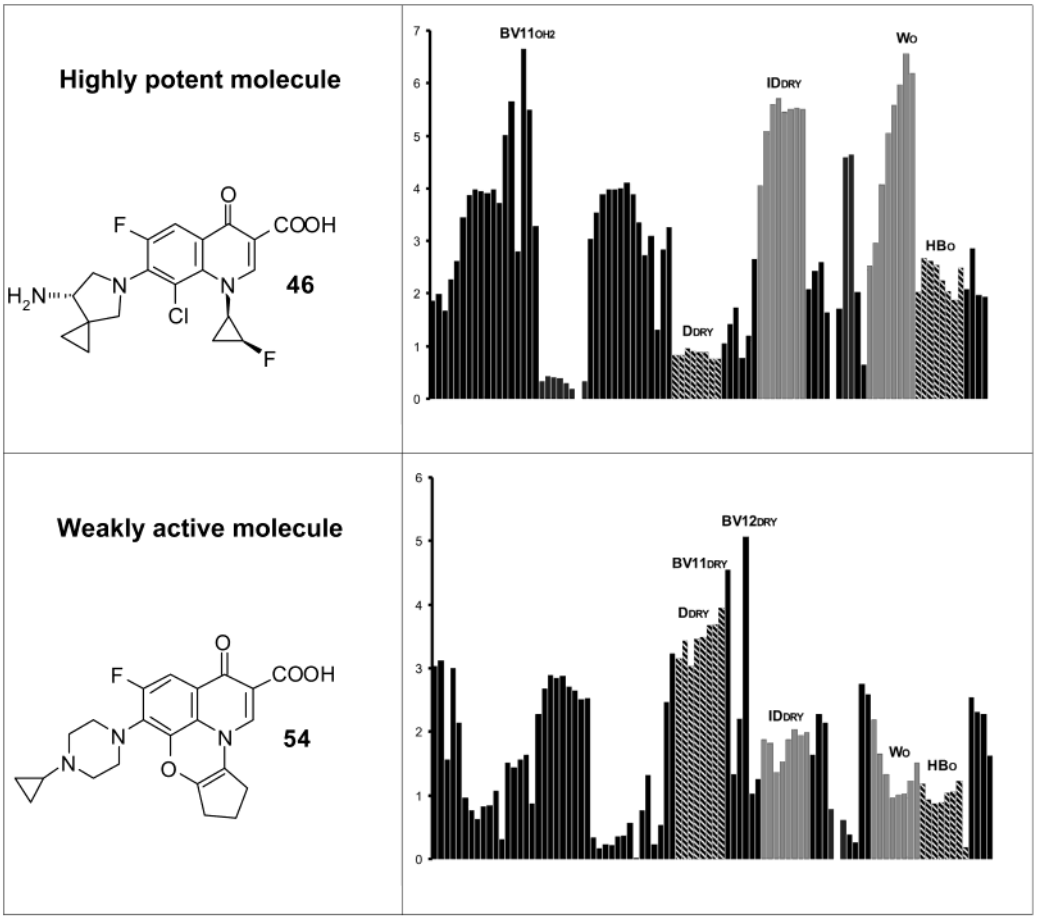

Figure 3. Comparison of the profile of VolSurf descriptors for a highly potent **46** and a weakly active compound **54**. High values of the best volume ($BV12_{OH2}$) of the water probe, high values of the integy moment (ID_{DRY}) of the lipophilic probe, and high values of the hydrophilic region (W_O) of the hydrogen bond acceptor probe, together with low hydrophobic interactions D_{DRY}, explain the high potency of compound **46**. The weakly active compound **54** exhibits the opposite behavior for these important descriptors.

obtained from GRID force field. This method is not sensitive to atom's overlap, and the resulting molecular shape is very precise. Moreover it is the shape "felt" by the receptor or by the biomolecular environment when interacting with the target molecule. Molecular shape function can be seen as a combination of steric vector

Table 2. Statistical Results of PLS Analysis[a]

	Escherichia coli		*Pseudomonas aeruginosa*		*Staphylococcus aureus*		*Enterococcus faecalis*	
				VolSurf Model				
components	5	3	5	5	5	2	5	3
descriptors	92	67	92	68	92	59	92	49
r^2	0.83	0.71	0.85	0.83	0.81	0.57	0.79	0.63
q^2	0.49	0.50	0.58	0.60	0.35	0.41	0.24	0.43
SDEP[65]	0.84	0.79	0.65	0.61	0.86	0.8	0.92	0.84
				GLOBAL Model				
components	3	3	3	3	3	3	3	3
descriptors	507	406	445	375	480	391	480	393
r^2	0.81	0.82	0.81	0.82	0.74	0.80	0.71	0.74
q^2	0.54	0.61	0.59	0.68	0.45	0.59	0.30	0.51
SDEP	0.76	0.76	0.67	0.69	0.71	0.63	0.77	0.72

[a] Results of the chemometric modeling are summarized. Regarding the number of components, r^2, q^2, and SDEP values the left-hand figures refer to results before and right-hand figures to results after fractional factorial design (FFD).

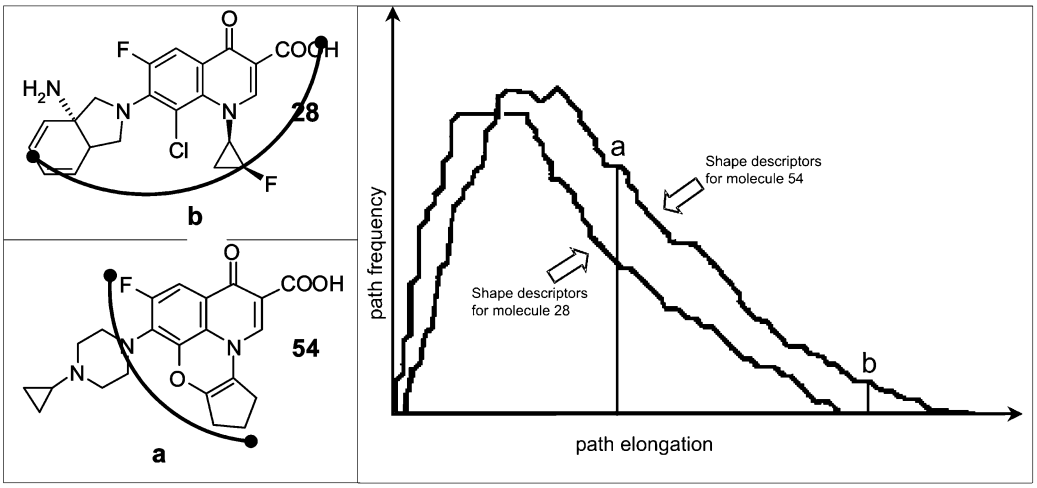

Figure 4. Schematic representation of the SHAPE descriptors for molecules **28** and **54**. The path elongations a and b reported in the histograms correspond to the different SHAPE-curvatures in molecules **54** and **28**.

descriptors with one extreme in the center of mass of a molecule and with the other located in the molecular surface. The "binned" distribution of such descriptors can be a very useful molecular shape function, and each bin can be considered an independent molecular shape descriptor. Histograms for two dataset molecules are shown in Figure 4.

SHAPE descriptors were pretreated using block-unweighted scales, merged with the VolSurf descriptors, and subjected to PLS analysis. The global model of this extended VolSurf approach is optimal with two components and exhibits a significantly improved statistical quality as compared to the results from the classical VolSurf approach; a marginally reduced r^2 value (0.75 versus 0.83) is more than compensated by a highly improved predictivity with a q^2 value of 0.63 versus 0.43. The overall quality of the global model, obtained with the extended VolSurf approach, is demonstrated in the plot of experimental versus calculated biological activities in Figure 5. The entire training set could be modeled without any significant outlier behavior.

Also for the extended VolSurf approach separate PLS models were derived for the four test systems to enable comparative statistical analysis (Table 2). Initial PLS analysis resulted in three-component models that explain 81% (*E. coli*, *P. aeruginosa*), 74% (*S. aureus*) and 71% (*E. faecalis*) of the variance in bactericidal activity. Improvement of model interpretation and predictivity by variable selection via FFD reduced the number of descriptors, as indicated in Table 2, and increased the q^2 values to 0.61 (*E. coli*), 0.68 (*P. aeruginosa*), and 0.59 for *S. aureus* and 0.51 for *E. faecalis*.

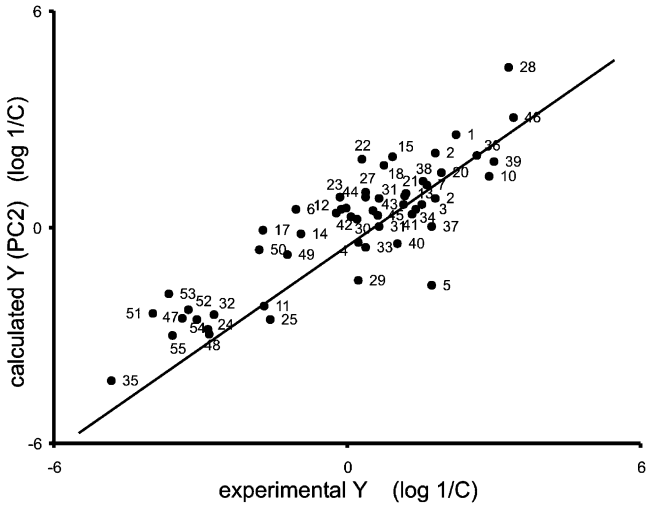

Figure 5. The overall quality of the global model, obtained with the extended VolSurf approach, is demonstrated in the plot of the experimental bactericidal activities (experimental Y) versus the data calculated with our model (calculated Y). The plot shows that the entire training set could be modeled without any significant outlier behavior.

A stringent proof of model quality is the external prediction of test set molecules. This was performed in the present study for seven quinolones, structures of

Chart 3. Chemical Structures of the Quinolone Test Set ($n = 7$)

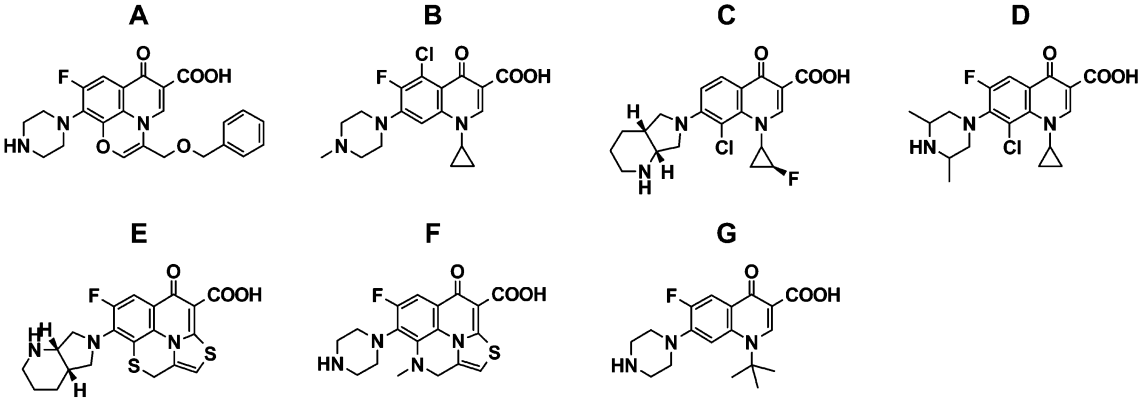

Table 3. Experimental Activity of the Test Set Compounds[a]

code	*Escherichia coli*	*Pseudomonas aeruginosa*	*Staphylococcus aureus*	*Enterococcus faecalis*
A	3.55	3.55	4.15	4.15
B	7.10	5.28	6.48	5.88
C	7.13	5.61	6.51	6.51
D	7.16	5.63	6.54	5.93
E	7.16	5.63	6.86	6.54
F	7.11	5.89	6.81	6.49
G	7.06	6.14	6.44	6.44

[a] Bactericidal activity is expressed as log 1/*C*.

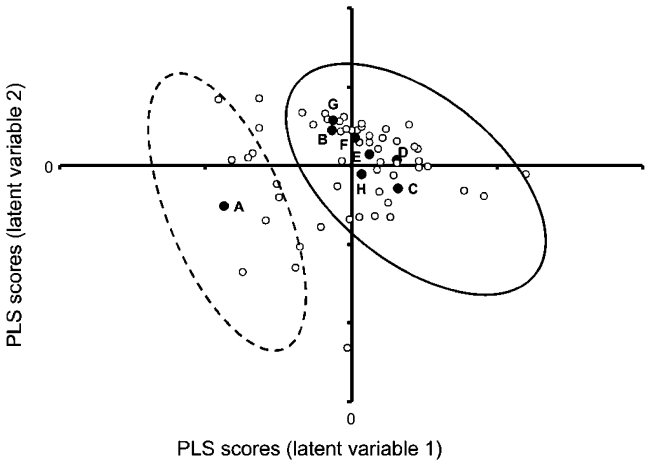

Figure 6. The PLS scores plot demonstrates the precise separation into highly (right-hand ellipse) and weakly active compounds (left-hand dashed ellipse). In addition, the precise prediction of seven test set molecules is indicated. Both the weak compound **A** and the potent compounds **B**−**G** are correctly projected in the corresponding regions.

which are given in Chart 3. Biological tests at Bayer company had indicated compound **A** to exhibit weak and compounds **B** to **G** to exhibit potent activity; the corresponding experimental log 1/*C* values for the four test systems are given in Table 3. The quality of the external prediction for the seven test set quinolones is graphically shown in a PLS scores plot (Figure 6). First of all this plot demonstrates the precise separation into highly (right-hand ellipse) and weakly active compounds (left-hand dashed ellipse) in accordance with the high statistical quality of the derived PLS model. In addition, this plot demonstrates the precise prediction of the seven test set molecules. Both the weak compound **A** and the potent compounds **B**−**G** are correctly projected in the corresponding regions.

Taken together, the application of an extended VolSurf approach, first described in this paper, yields a highly significant chemometric model for a training set of 55 quinolones without any outlier behavior. Predictivity of the PLS model could be demonstrated further by the correct prediction of external test set molecules. Structural requirements that arise from the analysis of the model are in very good agreement with previously published data.[24−26,36] Moreover this model was tested on molecules such as 30A[37] and 31B[37] that are characterized by a broad spectrum of activity against Gram-positive and Gram-negative bacteria. Activities of these molecules were adequately predicted.

Experimental Section

A. Databases. The training set comprises 55 quinolones (Chart 2) including the marketed moxifloxacin **02**, levofloxacin **03**, norfloxacin **04**, ciprofloxacin **05**, sparfloxacin **34**, lomefloxacin **44**, and pefloxacin **45**. The test set includes seven quinolones (Chart 3). All compounds were synthesized at Bayer AG, Wuppertal, Germany.[38−58] General aspects of quinolone chemistry can be found in Grohe[59] as well as Petersen and Schenke.[60]

B. Biological Tests. Biological data (Table 1) exclusively stem from Bayer AG, Wuppertal, Germany. Minimal inhibitory concentrations (MIC) against the aerobic pathogens were determined by standard agar dilution or broth microdilution method according to NCCLS guidelines (Methods for Antimicrobial Susceptibility Test for Bacteria That Grow Aerobically, National Committee for Clinical Laboratory Standards, Wayne, PA, M7-A5, Vol. 20, No. 2, 2001) using Mueller−Hinton (MH) agar or broth. *E. coli* and *P. aeruginosa* were used as examples for Gram-negative, *S. aureus* and *E. faecalis* for Gram-positive bacteria.

C. 3D-Structures Generation. Molecular models and geometry optimizations were performed using the software package SYBYL[61] running on a Silicon Graphics O2 workstation with operating system IRIX Release 6.5. Geometries of the molecules were optimized with the standard TRIPOS force field.[62] Conformational analysis was not performed because the structures used are mainly rigid and because of the relative independence of VolSurf descriptors from conformation of molecules.[63,64]

D. Chemical Descriptors. VolSurf Descriptors. VolSurf[63,64] is a computational procedure to produce 2D molecular descriptors from 3D molecular interaction energy grid maps. The basic idea of VolSurf is to compress the information present in 3D maps into a few 2D numerical descriptors which are very simple to understand and to interpret. VolSurf working examples are extensively reported.[65] By using multivariate statistics coupled with interactive 2D and 3D plots, valuable insights for drug design, PK profiling and screening are obtained. **SHAPE Descriptors**. The shape analysis approach is based on minimum paths and euclidean distances

calculated between pairs of grid points. The minimum path is the shortest path that connects two grid points lying on the molecular surface. Only positive GRID energy values are taken into account; 100 default grid points are selected according to an equidistribution criterion, to span the entire molecular surface. Paths and distances are calculated for all combinations between each of these 100 points and all the points of the molecular surface.

E. Statistical Analysis. Principal component,[66] fractional factorial design,[67] and PLS analyses were performed with the GOLPE software, version 3.09,[67] on Silicon Graphics workstations.

Acknowledgment. We would like to thank Dr. Uwe Petersen and Prof. Dr. Harald Labischinski, Bayer AG, Wuppertal, Germany, for helpful discussions and for providing the structures and the bactericidal activities of the training and test set quinolones.

References

(1) Hooper, D. C. Mechanisms of action of antimicrobials: focus on fluoroquinolones. *Clin. Infect. Dis.* **2001**, *32* (Suppl 1), S9−S15.
(2) Drlica, K.; Zhao, X. DNA gyrase, topoisomerase IV, and the 4-quinolones. *Microbiol. Mol. Biol. Rev.* **1997**, *61*, 377−392.
(3) Shen, L. L.; Chu, D. T. W. Type II DNA topoisomerases as antibacterial targets. *Curr. Pharm. Des.* **1996**, *2*, 195−208.
(4) Gootz, T. D.; Brighty, K. E. Chemistry and mechanism of action of the quinolone antibacterials. In *The quinolones*, 2nd ed.; Andriole, V. T., Ed.; Academic Press: San Diego, 1998; pp 29−80.
(5) Levine, C.; Hiasa, H.; Marians, K. J. DNA gyrase and topoisomerase IV: biochemical activities, physiological roles during chromosome replication, and drug sensitivities. *Biochim. Biophys. Acta-Gene Struct. Expr.* **1998**, *1400*, 29−43.
(6) Shen, L. L.; Mitscher, L. A.; Sharma, P. N.; O'Donnell, T. J.; Chu, D. T. W.; Cooper, C. S.; Rosen, T.; Pernet, A. G. Mechanism of inhibition of DNA gyrase by quinolone antibacterials: a cooperative drug−DNA binding model. *Biochemistry.* **1989**, *28*, 3886−3894.
(7) Palumbo, M.; Gatto, B.; Zagotto, G.; Palù, G. On the mechanism of action of quinolone drugs. *Trends Microbiol.* **1993**, *1*, 232−235.
(8) Fan, J. Y.; Sun, D.; Yu, H.; Kerwin, S. M.; Hurley, L. H. Self-assembly of a quinobenzoxazine-Mg^{2+} complex on DNA: a new paradigm for the structure of a drug−DNA complex and implications for the structure of the quinolone bacterial gyrase-DNA complex. *J. Med. Chem.* **1995**, *38*, 408−424.
(9) Lesher, G. Y.; Froelich, E. J.; Gruett, M. D.; Bailey, J. H.; Brundage, P. R. 1,8-Naphthyridine derivatives. A new class of chemotherapeutic agents. *J. Med. Chem.* **1962**, *5*, 1063−1068.
(10) Ball, P. The quinolones: history and overview. In *The quinolones*, 2nd ed.; Andriole, V. T., Ed.; Academic Press: San Diego, 1998; pp 1−28.
(11) Ball, P. Quinolone generations: natural history or natural selection? *J. Antimicrob. Chemother.* **2000**, *46*, 17−24.
(12) Kim, O. K.; Barrett, J. F.; Ohemeng, K. Advances in DNA gyrase inhibitors. *Exp. Opin. Invest. Drugs* **2001**, *10*, 199−212.
(13) Ball, P.; Fernald, A.; Tillotson, G. Therapeutic advances of new fluoroquinolones. *Exp. Opin. Invest. Drugs* **1998**, *7*, 761−783.
(14) Zhanel, G. G.; Ennis, K.; Vercaigne, L.; Walkty, A.; Gin, A. S.; Embil, J.; Smith, H.; Hoban, D. J. A critical review of the fluoroquinolones: focus on respiratory infections. *Drugs* **2002**, *62*, 13−59.
(15) Perry, C. M.; Balfour, J. A. B.; Lamb, H. M. Gatifloxacin. *Drugs* **1999**, *58*, 683−696.
(16) Barrett, J. F. Moxifloxacin Bayer. *Curr. Opin. Invest. Drugs* **2000**, *1*, 45−51.
(17) Lowe, M. N.; Lamb, H. M. Gemifloxacin. *Drugs* **2000**, *59*, 1137−1147.
(18) Bhavnani, S. M.; Ballow, C. H. New agents for Gram-positive bacteria. *Curr. Opin. Microbiol.* **2000**, *3*, 528−534.
(19) Hooper, D. C. Fluoroquinolone resistance among Gram-positive cocci. *Lancet Infect. Dis.* **2002**, *2*, 530−538.
(20) Bearden, D. T.; Danziger, L. H. Mechanism of action of and resistance to quinolones. *Pharmacotherapy* **2001**, *21*, 224S−232S.
(21) Piddock, L. J. V. Mechanisms of fluoroquinolone resistance: an update 1994−1998. *Drugs* **1999**, *58* (Suppl. 2), 11−18.
(22) Lietman, P. S. Fluoroquinolone toxicities. *Drugs* **1995**, *49* (Suppl. 2), 159−161.
(23) Ball, P.; Mandell, L.; Niki, Y.; Tillotson, G. Comparative tolerability of the newer fluoroquinolone antibacterials. *Drug Safety* **1999**, *21*, 407−421.
(24) Domagala, J. M. Structure−activity and structure-side-effect relationships for the quinolone antibacterials. *J. Antimicrob. Chemother.* **1994**, *33*, 685−706.
(25) Bryskier, A.; Chantot, J.-F. Classification and structure−activity relationships of fluoroquinolones. *Drugs* **1995**, *49* (Suppl. 2), 16−28.
(26) Gootz, T. D.; Brighty, K. E. Fluoroquinolone antibacterials: SAR, mechanism of action, resistance, and clinical aspects. *Med. Res. Rev.* **1996**, *16*, 433−486.
(27) De Sarro, A.; De Sarro, G. Adverse reactions to fluoroquinolones. An overview on mechanistic aspects. *Curr. Med. Chem.* **2001**, *8*, 371−384.
(28) Roychoudhury, S.; Ledoussal, B. Nonfluorinated quinolones (NFQs): new antibacterials with unique properties against quinolone-resistant Gram-positive pathogens. *Curr. Drug Targ.-Infect. Dis.* **2002**, *2*, 51−65.
(29) Li Q.; Mitscher, L. A.; Shen, L. L. The 2-pyridone antibacterial agents: bacterial topoisomerase inhibitors. *Med. Res. Rev.* **2000**, *20*, 231−293.
(30) Cecchetti, V.; Filipponi, E.; Fravolini, A.; Tabarrini, O.; Bonelli, D.; Clementi, M.; Cruciani, G.; Clementi, S. Chemometric methodologies in a quantitative structure−activity relationship study: The antibacterial activity of 6-aminoquinolones. *J. Med. Chem.* **1997**, *40*, 1698−1706.
(31) Llorente, B.; Leclerc, F.; Cedergren, R. Using SAR and QSAR analysis to model the activity of the quinolone-DNA complex. *Bioorg. Med. Chem.* **1996**, *4*, 61−71.
(32) Ohta, M.; Koga, H. Three-dimensional structure−activity relationships and receptor mapping of N1-substituents of quinolone antibacterials. *J. Med. Chem.* **1991**, *34*, 131−139.
(33) Gozalbes, F.; Brun-Pasquaud, M.; Garcia-Domenech, R.; Galvez, J.; Girard, P.-M.; Doucer, J.-P.; Derouin, F. Prediction of quinolone activity against Mycobacterium avium by molecular topology and virtual computational screening. *Antimicrob. Agents Chemother.* **2000**, *44*, 2764−2770.
(34) Cecchetti, V.; Tabarrini, O.; Sabatini, S.; Miao, H.; Filipponi, E.; Fravolini, A. Studies on 6-aminoquinolones: synthesis and antibacterial evaluation of 6-amino-8-methoxyquinolones. *Bioorg. Med. Chem.* **1999**, *7*, 2465−2471.
(35) Jaen-Oltra, J.; Salabert-Salvador, M. T.; Garcia-March, F. J.; Perez-Gimenez, F.; Tomas-Vert, F. Artificial neural network applied to prediction of fluoroquinolone antibacterial activity by topological methods. *J. Med. Chem.* **2000**, *43*, 1143−1148.
(36) Mitscher, L. A.; Devasthale, P.; Zavod, R. Structure−activity relationships. In: *Quinolone Antimicrobial Agents*, 2nd ed.; Hooper, D. C., Wolfson, J. S., Eds.; American Society for Microbiology: Washington, DC, 1993.
(37) Domagala, J. M.; Hagen, S. E.; Joannides, T.; Kiely, J. S.; Laborde, E.; Schroeder, M. C.; Sesnie, J. A.; Shapiro, M. A.; Suto, M. J.; Vanderroest, S. Quinilone Antibacterials Containing the New 7-[3-(1-Aminoethyl)-1-pyrrolidinyl] Side Chain: The Effects of the 1-Aminoethyl Moiety and Its Stereochemical Configurations on Potency and in Vivo Efficacy. *J. Med. Chem.* **1993**, *36*, 871−882.
(38) Takemura, M.; Kimura, Y.; Matsuhashi, N. EP 603,887, 1994; CAS Regist. No. 159877-30-2.
(39) (a) Petersen, U.; Bremm, K. D.; Dalhoff, A.; Endermann, R.; Heilmann, W.; Krebs, A.; Schenke, T. Synthesis and in vitro activity of BAY 12−8039, a new methoxyquinolone. 36th Interscience Conference on Antimicrobial Agents and Chemotherapy, New Orleans 1996, Abstact No. F1. (b) Dalhoff, A.; Petersen, U.; Endermann, R. In vitro activity of Bay 12−8039, a new 8-methoxy-quinolone. *Chemotherapy* **1996**, *42*, 410−425.
(40) (a) Atarashi, S.; Tsurumi, H.; Fujiwara, T.; Hayakawa, I. Asymmetric reduction of 7,8-difluoro-3-methyl-2*H*-1,4-benzoxazine. Synthesis of a key intermediate of (S)−(−)-ofloxacine (DR-3355). *J. Heterocycl. Chem.* **1991**, *28*, 329−331. (b) Atarashi, S.; Yokohama, S.; Yamazaki, K.; Sakano, K.; Imamura, M.; Hayakawa, I. Synthesis and antibacterial activities of optically active ofloxacin and its fluoromethyl derivative. *Chem. Pharm. Bull.* **1987**, *35*, 1896−1902.
(41) Koga, H.; Itoh, A.; Murayama, S.; Suzue, S.; Irikura, T. Structure−activity relationships of antibacterial 6,7- and 7,8-disubstituted 1-alkyl-1,4-dihydro-4-oxoquinoline-3-carboxylic acids. *J. Med. Chem.* **1980**, *23*, 1358−1363.
(42) (a) Grohe, K.; Zeiler, H. J.; Metzger, K.; (Bayer AG), DE 3,142,-854, 1981. (b) Zeiler, H. J.; Grohe, K. The in vitro and in vivo activity of ciprofloxacin. *Eur. J. Clin. Microbiol.* **1984**, *3*, 339−343. (c) Wise, R.; Andrews, J. M.; Edwards, L. J. In vitro activity of Bay 09867, a new quinoline derivative, compared with those of other antimicrobial agents. *Antimicrob. Agents Chemother.*

1983, *23*, 559−564. (d) Burnie, J.; Burnie, R. Ciprofloxacin. *Drugs Fut.* **1984**, *9*, 179−182. (e) Davis, R.; Markham, A.; Balfour, J. A. Ciprofloxacin. An updated review of its pharmacology, therapeutic efficacy and tolerability. *Drugs* **1996**, *51*, 1019−1074.
(43) Petersen, U., et al. EP 187,376., 1986
(44) Petersen, U., et al. EP-A 550,903, 1993.
(45) Petersen, U., et al. EP 523,512, 1993.
(46) Petersen, U., et al. EP 113,091, 1984.
(47) Petersen, U., et al. EP 350,733, 1990.
(48) Petersen, U., et al. EP-A 520,277, 1992.
(49) Petersen, U., et al. EP 705,828, 1996.
(50) Petersen, U., et al. EP 224,178, 1987.
(51) Miyamoto, T.; Matsumoto, J.; Chiba, K.; Egawa, H.; Shibamori, K.; Minamida, A.; Nishimura, Y.; Okada, H.; Kataoka, M.; Fujita, M.; Hirose, T.; Nakano, J. Pyridonecarboxylic acids as antibacterial agents. Part 14. Synthesis and structure−activity relationships of 5-substituted 6,8-difluoroquinolones, including sparfloxacin, a new quinolone antibacterial agent with improved potency. *J. Med. Chem.* **1990**, *33*, 1645−1656.
(52) Petersen, U., et al. EP 167 763, 1985.
(53) Wentland, M. P.; Bailey, D. M.; Cornett, J. B.; Dobson, R. A.; Powles, R. G.; Wagner, R. B. Novel amino-substituted 3-quinolinecarboxylic acid antibacterial agents: synthesis and structure−activity relationships. *J. Med. Chem.* **1984**, *27*, 1103−1108.
(54) Irikura, T.; et al. (Kyorin), Belgian Patent 887,574, 1980; *Chem. Abstr.* **1981**, *95*, 187096n.
(55) Itoh, Y. et al. *Chem. Abstr.* **1985**, *103*, 123517b.
(56) Goueffon, Y.; Montay, G.; Roquet, F.; Pesson, M. Sur un nouvel antibactérien de synthèse: l′acide éthyl-1-fluoro-6-(methyl-4-pipérazinyl-1)-7-oxo-4-dihydro-1.4-quinoléine-3 carboxylique (1589 R. B.). *C. R. Acad. Sci. Biol.* (Paris) **1981**, *292*, 37−40.
(57) Prous J.; Graul, A.; Castaner, J. DU-6859 (sitafloxacin). *Drugs Future* **1994**, *19*, 827−834.
(58) Schneide, S., et al. EP 563,732, 1993.
(59) Grohe, K. The chemistry of the quinolones: Methods of synthesizing the quinolone ring system. *Quinolone antibacterials*; Springer-Verlag: Berlin, Heidelberg, 1998; pp 13−62.
(60) Petersen, U.; Schenke, T. The chemistry of the quinolones: Chemistry in the periphery of the quinolones. *Quinolone antibacterials*; Springer-Verlag: Berlin, Heidelberg, 1998; pp 63−118.
(61) *Sybyl Molecular Modeling System*, version 6.8.1; Tripos Assoc.: St. Louis, MO.
(62) Vinter, J. G.; Davis, A.; Saunders, M. R. Strategic approaches to drug design. 1. An integrated software framework for molecular modeling. *J. Comput.-Aided Mol. Des.* **1987**, *1*, 31−55.
(63) Cruciani, G.; Crivori, P.; Carrupt, P.-A.; Testa, B. Molecular fields in quantitative structure-permeation relationships: the VolSurf approach. *J. Mol. Struct. (THEOCHEM)* **2000**, *503*, 17−30.
(64) Crivori, P.; Cruciani, G.; Carrupt, P.-A.; Testa, B. Predicting blood-brain barrier from three-dimensional molecular structure. *J. Med. Chem.* **2000**, *43*, 2204−2216.
(65) Mannhold, R.; Cruciani, G.; Weber, H.; Lemoine, H.; Derix, A.; Weichel, C.; Clementi, M. 6-varied benzopyrans as potassium channel activators: synthesis, vasodilator properties and multivariate analysis. *J. Med. Chem.* **1999**, *42*, 981−991.
(66) Wold, S.; Esbensen, K.; Geladi, P. Principal component analysis. *Chem. And Intell. Lab. System* **1987**, *2*, 37−52.
(67) Baroni, M.; Costantino, G.; Cruciani, G.; Riganelli, D.; Valigi, R.; Clementi, S. Generating Optimal Linear PLS Estimations (GOLPE): An advanced chemometric tool for handling 3D-QSAR problems. *Quant. Struct.-Act. Relat.* **1993**, *12*, 9−20.

JM030986Y